

Raman spectra in epitaxial thin films $La_{1-x}Ca_xMnO_3$ ($x = 0.33, 0.5$) grown on different substrates

Y. M. Xiong^a, T. Chen^a, G. Y. Wang^a, X. H. Chen^{a,b*} and X. Chen^b and C. L. Chen^{b†}

*a) Structure Research Laboratory and Department of Physics,
University of Science and Technology of China,
Hefei, Anhui, 230026, P. R. China*

*b) Texas Center for Superconductivity and Advanced Materials and Department of Physics,
University of Houston, Houston, Texas 77204*

(Dated: September 11, 2018)

Raman spectra of LCMO films grown on LAO (001), STO (001), and MgO (001) substrates were studied at different temperatures. The effect of temperature, doping level and strain on Raman spectra are discussed in detail. With decreasing temperature, the changes of Raman spectra are correlated with the disorder-order transition, such as: paramagnetism to ferromagnetism, and charge-ordering. The strain induced by lattice-substrate mismatch affects the Raman spectra strongly. The mode induced by disorder of oxygen defects is apparently observed in $La_{0.67}Ca_{0.33}MnO_3$ film on STO due to the larger tensile strain. While this mode can not be seen in the Raman spectra for the films on LAO and MgO. A strong unsigned mode at about 690 cm^{-1} is observed in all films except for $La_{0.67}Ca_{0.33}MnO_3$ film on LAO, which is not observed in bulk sample easily. It suggests that the mode is closely related to the strain.

PACS numbers: 78.30.-j, 75.47.Gk, 68.60.Bs

I. INTRODUCTION

Recently, $R_{1-x}A_xMnO_3$ ($R =$ rare earth, $A =$ Ca, Sr, or Ba) compounds have attracted much attention because of their colossal magnetoresistance (CMR)^{1,2,3,4}. Particularly, $La_{1-x}Ca_xMnO_3$ has a very rich phase diagram of ground states with competing order parameters^{5,6}. The parent compound is $LaMnO_3$, which belongs to the family of rotationally distorted perovskites⁷ and is an anti-ferromagnetic (AFM) insulator. With the increase of doped Ca^{2+} content, CMR has been observed in the Ca concentration of 0.2-0.5⁸. In this doping range, the compound transfers from a paramagnetic-insulator (PI) to a ferromagnetic-metal with decreasing temperature. For the high doping range with $0.5 \leq x \leq 0.875$, the doped charge carriers are localized and ordered with stripe modulations at low temperature^{9,10,11}. The compound at the phase boundary with $x = 0.5$ undergoes first a FM transition, and a simultaneous AFM and charge ordering (CO) transition at low temperature. Thus, it is representative and important to investigate the properties of compounds which are optimal doping for Curie temperature (T_c) ($x = 0.33$) and the phase boundary doping ($x = 0.5$).

A competition between Super-Exchange (SE)¹² and Double-Exchange (DE)¹³ interactions has long been used to explain the resulting spin alignment and transport properties of these manganese oxides. In addition, the strong electron-phonon coupling was found to play an

important role in the mechanism of CMR^{14,15}. In particular, the Jahn-Teller (JT) effect affects both the magnetic and transport properties in $La_{1-x}Ca_xMnO_3$ (LCMO) system^{14,15,16}. There are two types of distortions of the ideal perovskite structure in bulk samples. One is the rotational-like distortions of the MnO_6 octahedra due to the mismatch between the averaged ionic radii r_A of the A-site species and the ionic radius r_{Mn} of Mn. It is one of the strain effects induced by chemical pressure^{17,18}. The other is JT distortions of $Mn^{3+}O_6$ octahedra. It is a strong electron-phonon coupling. The strain can also be caused by the lattice-substrate mismatch^{1,19}. This kind of epitaxial strain is different from the strain induced by hydrostatic²⁰ or chemical pressure^{17,18}, since an in-plane strain generally accompanies an out-of-plane strain with different sign, which can cause new electronic behavior did not found in bulk materials of the same chemical composition¹. The interplay between substrate and film allows the modification of properties and can even enhance the magnetoresistive effect^{5,21}. This suggested a possible device applications with these films based on the sensitivity to magnetic fields²². There are two mechanisms by which substrates modify film properties. The first one is associated with the lattice distortion of epitaxially grown films. The substrate induces both bulk and biaxial strains in the film, which alters the physical properties of films^{23,24,25,26}. The other one is associated with the dynamics of film growth and the manner of strain release¹⁹, which induce phase separation and inhomogeneities in films^{27,28}. These suggest that the interesting phenomena maybe observed in highly strained thin films of manganite. So we grew films on substrates with different lattice parameters, and investigated the change of their properties to study the effect of strain

*Corresponding author, Electronic address: chenxh@ustc.edu.cn

†Corresponding author, Electronic address: cchen@uh.edu

induced by substrate.

Raman scattering was proved to be a useful tool for the study of various vibration and electronic excitations, phase transitions, lattice distortions, etc.. Thus, this technique affords a means by which energy and symmetry information regarding phonon, electron, and spin excitations can be simultaneously explored. It is well known that there are no Raman-active of lattice vibrations in the ideal cubic perovskite, all phonon modes originate from lattice distortions. Therefore, we can use Raman spectroscopy to study the lattice distortions in LCMO films which induced by the change of temperature and the strain comes from lattice-substrate mismatch. In addition, there are seldom work has been done on Raman spectra of the thin films with composition of 0.5.

In order to study the effect of strain systemically, LCMO films were deposited on (001) $LaAlO_3$ (LAO), (001) $SrTiO_3$ (STO), and (001) MgO (MgO) substrates, respectively. The strain in each film is different because the lattice parameters of these substrates are different. We investigated the Raman scattering in these films at different temperatures to study the change of phonon vibration induced by temperature, lattice-substrate mismatch and Ca concentration.

II. EXPERIMENTS

Thin films of $La_{1-x}Ca_{0.33}MnO_3$ ($x = 0.33$ and 0.5), about 200-300 nm in thickness, were grown on $LaAlO_3$ (001), $SrTiO_3$ (001), and MgO (001) substrates by pulsed laser deposition. The films were deposited at 800 °C in 400 mTorr oxygen partial pressure without subsequent post-annealing. The x-ray diffraction (XRD) measurements were carried out in Rigaku D/max- γ A x-ray diffractometer with graphite monochromatized $Cu K\alpha$ radiation ($\lambda=1.5406\text{\AA}$). Raman spectra were obtained on a LABRAM-HR Confocal Laser MicroRaman Spectrometer using the 514.5 nm line from an argon-ion laser. The data were fitted with Lorentzian function. The magnetic susceptibility measurement was carried out with a superconducting quantum interference device magnetometer(MPMS-5). The high pressure oxygen anneal were carried out in High Pressure Oxygen Furnace (Morris Research) at 195 atm and 500 °C for 24 hours.

III. RESULTS AND DISCUSSION

Figure 1 shows XRD pattern for films grown on three substrates with $x = 0.33$ and 0.5 . We labelled $La_{0.67}Ca_{0.33}MnO_3$ as LCMO1 and $La_{0.5}Ca_{0.5}MnO_3$ as LCMO2, respectively. The films were of single phase and highly crystallized as seen from the sharp and intense diffraction peaks. Generally, at the best growth conditions, the single-crystalline can be obtained in orthorhombic structure with the space group of Pnma due to the tilting of MnO_6 octahedra. In the films, the orien-

tation of the orthorhombic axes in respect of the interface depends on the type of the substrate^{27,29}. It has been found that LCMO1 films were [110] oriented on LAO substrate and mixed [001] and [110] oriented on STO substrate²⁷. Because the splitting between the (110) and (002) reflection of orthorhombic LCMO is too small to be resolvable (see JCPD No. 49-0416), the peaks of the films are indexed based on the single perovskite unit cell. According to the XRD data, we calculated the out-of-plane lattice parameters of films and substrates and listed them in the Table I. These results are consistent with the data reported in previous references^{23,30,31,32}. As shown in Table I, the lattice parameter of $LaAlO_3$ is 3.7916 Å, smaller than the lattice parameters of bulk crystals value of 3.86 Å for $La_{0.67}Ca_{0.33}MnO_3$ (LCMO1)^{31,33} and 3.84 Å for $La_{0.5}Ca_{0.5}MnO_3$ (LCMO2)³². Thus, the lattices of films on LAO undergo a simultaneous in-plane compression and an out-of-plane elongation due to the in-plane compressive strain induced by LAO substrate. In contrast, lattices of films grown on STO should undergo an in-plane tensile strain accompanying by a shrinkage along the out-of-plane orientation because its lattice parameter (3.9026 Å) is larger than the bulk value. It has been reported that the lattice-substrate mismatch affects the Mn-O bond length slightly in epitaxial LCMO films grown on different substrate, the change of Mn-Mn interatomic distance is controlled by altering the Mn-O-Mn angle²⁶. Thus, the in-plane compression and out-of-plane elongation of films on LAO are mainly achieved by the out-of-phase rotation of MnO_6 octahedra. The same is true of the films on STO, the lattice distortion of films on STO is also achieved by the out-of-plane rotation of MnO_6 octahedra.

It is expected that the out-of-plane lattice parameters of LCMO films grown on MgO should be smaller than that of films grown on STO, because the lattice parameter of MgO is larger than that of STO. While, it is interesting to note that the lattice parameters for the films grown on MgO are very close to the values from the LCMO bulk materials(see Table I). The Raman spectra also indicate that no strong strain effect appears in the MgO samples. These phenomena probably result from the strain-relieving mosaics³⁴ that has recently been discovered from the CeO_2 thin films on (001) MgO ³⁵. Theoretically, if the lattice mismatch is sufficiently large, a coincidence lattice can be formed to accommodate the large strain through slightly rotating film relative to the substrate. This rotational mismatch allows the film to assume its bulk lattice parameter and structure for resulting in a quasi-epitaxial behavior. Details about the mechanisms are under studied and will report later on. It is noticed that the out-of-plane lattice parameter increases when Ca concentration changes from 0.33 to 0.5 in the films grown on LAO. While in those grown on STO and MgO, their out-of-plane lattice parameters decrease. It may be induced by the different strain in each sample. The discussion on it will be carried out in detail later. In the following, we will discuss the effects of tempera-

ture, lattice-substrate mismatch and doping on Raman spectra.

Figure 2 and 3 show the Raman spectra of LCMO films with Ca concentration of 0.33 and 0.5 on three substrates at the temperatures of 293, 260, 240, 220, 200, 180, 160, 140, and 100 K, respectively. It is shown that the Raman modes are mainly located in three intervals at about $220\sim 250\text{ cm}^{-1}$ (ω_1), $450\sim 520\text{ cm}^{-1}$ (ω_2), and $610\sim 720\text{ cm}^{-1}$ (the lower frequency mode is labelled as ω_3 and the higher frequency mode is labelled as ω_4). ω_1 belongs to $A_g(2)$ mode (rotational mode), and is proportional to the angle of long-rang coherent static tilt of MnO_6 octahedra. The higher frequency modes ω_2 and ω_3 are assigned to JT-active vibrations. ω_2 belongs to $A_g(3)$ mode (bending mode) which is determined by the mean distance between La/Ca and apical oxygens. According to previous reports, ω_3 with $B_{2g}(1)$ symmetry is an in-phase oxygen stretching^{36,37,38}. Podobedov et al³⁸. considered this band is a disorder-induced Raman feature and expect its origin to reside in a lattice defect due to an existing oxygen deficit. This conclusion is supported by the less intensity of about 600 cm^{-1} band in annealed samples³⁸. Malde et al.³⁹ observed that the frequency of this mode shifts with the variation of annealing oxygen partial pressure. This seems to support the origin of this mode from the oxygen deficit. The relative intensity of this disorder-induced Raman band may serve as a good indication of the oxygen deficit in LCMO³⁸. In other articles^{37,40,41,42}, these authors believe this band from the JT distortion of MnO_6 octahedra. Therefore, it is necessary to study the origin of the 600 cm^{-1} mode.

According to previous report in $La_{0.67}Ca_{0.33}MnO_3$ film on LAO³⁸, a higher frequency mode at about 660 cm^{-1} comes from the degradation of the sample surface area. While the strong peaks at about 690 cm^{-1} and the weak band at about 610 cm^{-1} in our samples are inconsistent to the results reported by Podobedov et al³⁸. In order to confirm the origin of the two peaks, we annealed our samples in high pressure oxygen. Because the two peaks are weak in Raman spectra of LCMO1/LAO, it is hard to distinguish the annealing effect. We compared the Raman spectra of LCMO1 films on STO and MgO, and LCMO2 on LAO. Figure 4 shows the Raman spectra of as-grown and annealed LCMO1 films on STO and MgO, and LCMO2 film on LAO, respectively. These samples were annealed in high pressure oxygen at 195 atm and $500\text{ }^\circ\text{C}$ for 24 hours. As shown in Fig. 4, for the intensity of ω_4 , no obvious weakening can be observed after annealing, even it increases in LCMO1/MgO. Thus the potential origin of ω_4 from oxygen deficit could be incorrect. ω_4 is unsigned and unfamiliar in Raman spectra of LCMO samples. Detailed discussions are carried out later. In our samples, the change of ω_3 is hardly distinguished because of the weaker relative intensity than ω_4 . In the bottom panel of Fig.4, there is a weak peak at about 610 cm^{-1} in as-grown LCMO2/LAO. After annealing in high pressure oxygen, this peak disappears. It may indicate a decrease of oxygen deficit. Therefore,

our results seem to support the origin of 600 cm^{-1} from the oxygen deficit. However, no apparent change for ω_3 is observed in LCMO1/STO after annealing in high pressure oxygen. It suggests that the oxygen deficit in LCMO1/STO is very stable due to a large tensile strain. Thus, we believe the mode at about 600 cm^{-1} is correlated with the oxygen deficit and affected by the strain strongly.

A. Effect of Temperature

In the Fig.2, the Raman spectra of $La_{0.67}Ca_{0.33}MnO_3$ films were measured at the temperatures of 293, 260, 240, 220, 200, and 100 K. In Raman spectra of LCMO1/LAO film, a much sharp peak appears at about 486 cm^{-1} , and this feature is almost unchanged with changing temperature. Compared with the Raman spectra of LAO substrate³⁷, this sharp peak is attributed to LAO substrate, identified by asterisks(*). The Raman spectra feature from film near 480 cm^{-1} is broad and hardly distinguished because of the overlap of peaks from film and LAO substrate. The high frequency modes ω_3 and ω_4 of film grown on LAO are weak, and temperature dependence of frequency shift can not be observed clearly. In bulk samples with Ca concentration in the region of $0.3 < x < 0.4$, the ω_3 mode is weak. The weakening of this mode can be correlated with the reduction of JT distortion, introduced by the presence of Ca⁴¹. In the film grown on LAO, Raman spectra are similar to those in bulk samples. The high frequency modes are weak due to the present of Mn^{+4} ions which is JT inactive. Figure 5 shows temperature dependence of the frequency shift of Raman modes for LCMO1 films. In the Fig. 5a, the ω_1 mode for LCMO1/LAO hardens with decreasing temperature. In earlier reports, there is one mode in this frequency range for LCMO samples^{37,43,44}, and it is with $A_g(2)$ symmetry and attributed to the rotation of MnO_6 octahedra. In the film on LAO, the MnO_6 octahedra rotate to match the distortion of lattice induced by lattice-substrate mismatch. At room temperature, the in-plane shrink and out-of-plane elongation of lattices is achieved by the rotation of MnO_6 octahedra. With decreasing temperature, the hardening of ω_1 , indicating the increase of tilt angle of MnO_6 octahedra, is maybe caused by the increase of lattice-substrate mismatch. The peak of ω_1 sharpens slightly below 220 K. As shown in the inset of Fig.2a, the magnetic phase transition can be observed clearly, the Curie Temperature (T_C) is about 220 K. The sharpening of ω_1 peak has been reported earlier by Podobedov et al³⁸ and attributed to the spin-lattice coupling in the spin-ordered FM state. Recently, another explanation of this narrowing of ω_1 , could be the increase of long range structural coherence due to the reduction of the dynamic JT distortion^{37,45}.

According to the previous reports, the Raman feature ω_2 could contain several peaks with different symmetry^{36,43,46}, its temperature dependence is com-

plex due to the overlap of these modes. The different temperature behaviors of these modes induce a shift of the broad ω_2 band. As shown in Fig. 2a, with decreasing temperature some much sharp peaks appear and their intensities become more strong at the temperatures below T_C . This is consistent with that reported in $La_{0.7}Ca_{0.3}MnO_3$ /LAO film³⁷. The 441.4 cm^{-1} line is classified to the bending E_g mode for rhombohedral $La_{0.93}Mn_{0.98}O_3$ ⁴³. These sharp peaks may be correlated with the electron or spin excitations existing in the metallic-state phase. Recently, another explanation was reported that these much sharper Raman lines corresponding to the Γ -point Raman phonon of the ordered structure reflects the disorder-order transition, concomitant with the PM to FM and insulator-metal transitions⁴⁶. However, no sharp peaks appear when the sample enters FM state in the film on STO. In addition, because the E_g modes always appear in rhombohedral symmetric structure^{43,47}, the appearance of these sharp peaks maybe indicate a structure transition from orthorhombic lattice to rhombohedron. These sharp peaks in the $400\text{ to }450\text{ cm}^{-1}$ range at low temperatures also appears in bulk samples with composition of about 0.33⁴¹. This indicates that a compressive strain can not affect the evolution of lattice with decreasing temperature. While a tensile strain affects the lattice strongly. These sharp peaks in the $400\text{ to }500\text{ cm}^{-1}$ range always appear together in the Raman spectra of LCMO^{37,41,43,45,46}. Based on their similar behavior with the temperature and substrates in our case and the earlier reports in films and bulk samples^{37,41}, we attribute these narrow peaks to the same symmetry.

The LCMO1 film grown on STO undergoes a tensile strain, whose Raman spectra are shown in the Fig. 2b. The in-plane lattice expands due to the tensile strain, at the same time out-of-plane lattice shrinks. This kind of anisotropic distortion of lattices should induce the tilt of MnO_6 octahedra. The frequency of ω_1 mode decreases with decreasing temperature which may be induced by decreasing tilt angle of MnO_6 octahedra due to the reduction of lattice-substrate mismatch (see Fig. 5a). The intensity of ω_1 increases apparently above 240 K, and decreases dramatically with the decrease of temperature below 240 K. In contrast, the full width at half maximum (FWHM) decreases firstly above 240 K, then increases with decreasing of temperature. The strongest intensity of ω_1 mode at 240 K indicates a strongest static JT distortion at this temperature. The dramatic decrease of intensity below 240 K should be induced by spin-lattice coupling in spin-ordered FM state. As shown in Raman spectra of LCMO1 film grown on STO, ω_2 is absent at room temperature, then appears and becomes more obvious at low temperature. These changes are caused by the increase of MnO_6 octahedra bending at the low temperatures. The frequencies of ω_2 and ω_3 , which are correlated with JT distortion, shift up as temperature decreases. This is induced by lattice shrink due to the decrease of temperature. As shown in Table I, the out-of-plane lat-

tice parameter of film grown on STO is the least, which indicates the stretching of in-plane lattices. Therefore, the mean distance between La/Ca and apical oxygens is larger than that in bulk sample. With decreasing temperature, the distance between La/Ca and apical oxygens decreases continually, which leads to an hardening of the frequency in ω_2 . As shown in the Fig.2b, the intensities of ω_2 and ω_3 , increase with decreasing temperature compared with ω_1 . It is due to the change from small-polaron-dominated transport in the paramagnetic (PM) phase to large-polaron (metallic) transport in the FM phase⁴⁸. No obvious change in ω_4 is observed when the sample enters FM state. It suggests that ω_4 is independent of the PM to FM transition.

In the spectra of LCMO1/MgO, the frequency of ω_1 hardens slightly with lowering temperature. According to the XRD pattern (see Fig. 1), the lattice-substrate mismatch is slight in film on MgO. In addition, the intensity of ω_1 in LCMO1/MgO increases above 220 K, reaches the maximum at 220 K, then decreases dramatically. This behavior is similar to the case of LCMO1/STO and may be correlated with the PM to FM transition, as observed in Raman spectra of LAMO1/STO. ω_2 feature hardens with decreasing of temperature above 220 K, then softens again (see Fig. 2c). These phenomena may be due to the coexistence of several modes in this interval. These modes have different temperature behaviors because of their different symmetry. As previously reported in $RMnO_3$ (R = Ca, Pr, Nd, Tb, Ho, Er and Y) samples, this feature contains the bending and antisymmetric stretching modes³⁶. The frequency of antisymmetric (AS) stretching mode simply depends on the Mn-O bond length. The frequency of bending mode strongly depends on the mean value of the shortest distance between La/Ca ion and apical oxygen. With decreasing temperature, the Mn-O bond length shrinks slightly, while the La/Ca-O distances change obviously. Thus, these different temperature effect of each mode induce a complex behavior of ω_2 feature. As shown in Fig. 2c, ω_3 band can not be observed, which indicates a little oxygen deficit in this film.

In the Fig. 3, the Raman spectra of $La_{0.5}Ca_{0.5}MnO_3$ films are shown at the temperatures of 293, 250, 200, 180, 140, 100, and 83 K, respectively. The bulk LCMO sample with Ca concentration of 0.5 is at the phase boundary between FM and charge ordered AF state. According to the previous report⁴³, with decreasing temperature a competition between the ferromagnetic and antiferromagnetic ordering occur. In a narrow region ($0.44 < x < 0.54$) upon cooling, the compound becomes first ferromagnetic, then antiferromagnetic, in particular, for $x = 0.5$, $T_C = 225 \sim 265\text{ K}$, $T_N = 130 \sim 160\text{ K}$. Below T_N orbital and charge ordering takes place and a superstructure of $P2_1/m$ symmetry is formed supported by the much richer Raman spectra feature in this sample than that of orthorhombic $LaMnO_3$ ⁴⁹. In the Raman spectra of LCMO2 film on LAO, the peak at about 486 cm^{-1} is from LAO substrate, identified by asterisks. The frequency of ω_1 hard-

ens with decreasing temperature (see Fig. 6) due to the increase in tilt angle of MnO_6 octahedra, as observed in LCMO1 film. At the same time, the intensity of ω_1 increases slightly above 180 K, then decreases continuously with decreasing temperature. At low temperature, several additional peaks present at 425, 446, and 469 cm^{-1} in LCMO2 on LAO. Similar spectral shape at low temperature has been reported in bulk $La_{0.5}Ca_{0.5}MnO_3$ by Iliev et al.⁴³ and Abrashev et al.³². It is believed that the presence of these sharp peaks is induced by the lowering symmetry as samples enter CO state. The peak of ω_3 mode is weak and can not be observed clearly. This weakening of disorder-induced band does not indicate a less oxygen deficit in LCMO2. It has been reported in bulk samples that the distorted volume reaches its maximum for disordered Mn^{3+}/Mn^{4+} composition with $\sim 30\%$ Mn^{4+} .⁴⁶ The decrease in intensity of the disorder-induced bands at higher doping and the appearance of some sharp Raman features can be explained by increasing the volume of domains with short-range charge/orbital-ordered³². As reported in bulk sample of $La_{0.5}Ca_{0.5}MnO_3$, Raman structures are weak at room temperature, the structure at ~ 480 and ~ 600 cm^{-1} develop and become strong with decreasing temperature below CO temperature.^{32,43,50} Compared with the bulk sample, the Raman spectra is similar to that for bulk sample except that obvious peaks appear at ~ 235 and ~ 690 cm^{-1} at room temperature. With decreasing temperature, the intensity of the mode at ~ 480 cm^{-1} increases and the Raman shift shows a systematical change. However, no apparent peak at ~ 600 cm^{-1} is observed with cooling the temperature to 83 K. The different spectra from bulk sample could arise from the strain induced by the lattice mismatch between the film and substrates. In addition, the peak of ω_4 enhances and hardens gradually with decreasing temperature and no obvious change is seen when the sample enters charge ordering state.

The temperature dependence of Raman spectra for LCMO2/STO are shown in Fig. 3b. The intensity of ω_1 increases above 160 K, then decreases dramatically below 160 K as temperature decreases. At the same time, the frequency of this mode softens first slightly with decreasing temperature, then hardens below 160 K (see Fig. 6). The decrease in intensity of ω_1 below 160 K is contrary to the previous report in bulk samples^{32,50}. In bulk samples, the modes enhance as the system enters CO state due to the lowering symmetry. Thereby, the anomalous change in the intensity of ω_1 should be induced by the strain. In additional, the anomalous change only occurs in the band of ω_1 . It suggests that the strain effect affects the tilt angle of MnO_6 octahedra strongly. ω_2 becomes obvious and narrow gradually with decreasing of temperature. The slight hardening of ω_2 implies that the distance between La/Ca and apical oxygens shrinks slightly. The frequencies of high frequency modes increase with decreasing temperature due to the compression of lattices. The mean distance between La/Ca and apical oxygens and the length of Mn-O bond are elongated fully in the

plane parallel to the substrate. Therefore, the lattices shrink continually as temperature decreases, then all high frequency modes shift up.

In LCMO2/MgO sample, ω_1 is broad and weak, and weakens with lowering temperature. It implies that there are a small quantity of tilted MnO_6 octahedra in this sample, which become much less with decreasing temperature. According to the XRD pattern, the lattice distortion of film on MgO is the least. The lack of tilted MnO_6 is consistent with this result. The change of ω_2 is similar to that in LCMO1 film on MgO and the temperature corresponding to the strongest intensity is 140 K. The reason is the same as that in the case of $x = 0.33$. The intensity of ω_4 increases continuously to the maximum, and FWHM narrows to the minimum at 100 K. Then the intensity decreases dramatically.

In summary, we discussed the variation of Raman spectra of LCMO films with changing temperature in this part. Although, they were deposited on the different substrates, their Raman spectra are all correlated with the transition of magnetic phase from disorder to order. These transitions usually are accompanied by the change of Jahn-Teller distortion. With decreasing temperature, the Raman spectra change obviously at the phase transition temperature. ω_1 mode, which is correlated with the tilt angle of MnO_6 octahedra, hardens or softens with lowering temperature due to the change of lattice-substrate mismatch. As samples enter the ordered FM state, the peak of ω_1 band sharpens in LCMO1/LAO due to the increase of spin-lattice coupling. In LCMO1 on STO and MgO, the intensity of ω_1 decreases dramatically because of the spin-lattice coupling too. ω_2 and ω_3 are correlated with JT distortion. The behavior of ω_2 feature is complex due to the coexistence of several modes. These modes with different symmetry have different behavior with lowering temperature. As previous report³⁶, in this interval, the bending mode would change obviously, while the stretching mode would change slightly as temperature decreases. ω_3 is a indicator of oxygen deficit in LCMO1 films and weakens in LCMO2 films due to the increasing the volume of domains with short-range charge/orbital-ordered³². ω_4 does not arise from oxygen deficit in films. Detailed discussions about this mode are carried out later.

B. Effect of the Lattice-Substrate Mismatch

To study the effect of strain in these films, we compare the Raman spectra of films on different substrates. As shown in Fig. 2, there are four main peaks centered at the frequency about 228, 450, 625 and 675 cm^{-1} in all films. At room temperature, the frequency of ω_1 in the films on MgO is less than that of STO, and that of LAO is least (see fig. 5). With the change of the mismatch between film and substrate, the lattices of film undergo an in-plane elongation (compression) and a simultaneous out-of-plane compression (elongation). In the film

on STO, the frequency of ω_1 is the largest one due to the larger tensile strain in this film. With decreasing temperature, ω_1 softens in LCMO1/STO film, while it hardens in LCMO1/LAO film. The thermal expansion coefficients of LCMO films are not available. The thermal expansion coefficients of LAO ($1 \times 10^{-5} K^{-1}$), STO ($0.9 \times 10^{-5} K^{-1}$), and MgO ($1.1 \times 10^{-5} K^{-1}$) are close to each other²³, the thermal expansion contribution to the lattice distortions should be similar for the films on three substrates. To explain the contrary shift of ω_1 band in the films on different substrate, it is reasonable that we assume the thermal expansion coefficients of substrates are larger than that of the film. In LCMO1/LAO film, the lattice mismatch increases with decreasing temperature due to the above assumption. Thus, the tilt of MnO_6 octahedra is harder at low temperature. In LCMO1/STO film, the mismatch decreases as temperature decreases. ω_1 hardens slightly in film on MgO with decreasing temperature due to the slight strain in this film at room temperature. Therefore, the tilt angle of MnO_6 octahedra is partly affected by the strain in LCMO1 films. In LCMO1 film on STO, no peak appears around $480 cm^{-1}$ at room temperature. It implies that there is no MnO_6 octahedra bending or the banding mode is too weak to be observed. In addition, there are no additional sharp peaks appear in the films on STO and MgO at low temperature. While these sharp peaks appeared in the 400 to $450 cm^{-1}$ range at low temperature are observed in film on LAO and $La_{0.67}Ca_{0.33}MnO_3$ bulk samples⁴¹. It proves that these much sharp peaks are determined by the lattice distortion, which can be modified by the type of strain. According to the above discussion, only in-plane compressive strain could induce a structural transition from orthorhombic lattice to rhombohedron. As shown in Fig. 2 and Fig. 3, both the ω_2 band in films on MgO hardens above a certain temperature and softens below this temperature, no similar behavior is observed in films on LAO and STO. Thereby, it suggests that this complex frequency change of ω_2 depend on the type of substrates strongly. In the region of ω_2 band, the various modes coexist. Each mode with different symmetry should be affected by strain differently. In the films on LAO and STO, the effect of strain induces the monotonic change of frequency. While in the films on MgO, the strain effect is not dominant.

At high frequencies, the LCMO1/LAO sample has a broad peak at about $670 cm^{-1}$, which contains two peaks. The lower frequency mode is correlated with the oxygen deficit in the films and may serve as a good indicator of the oxygen deficit in LCMO³⁸. The strong intensity of this mode in LCMO1/STO film indicates that the oxygen deficit is the largest in film with tensile strain. As shown in Fig. 4, in the bottom panel, there is a weak peaks at about $610 cm^{-1}$ for as-grown LCMO2/LAO film. After annealing in high pressure oxygen, this peak disappears. It may indicate a decrease of oxygen deficit induced by the annealing process. In the top panel of Fig. 4, the ω_3 mode is unchanged after annealing. It sug-

gests that the lattice defects in LCMO1/STO film are intrinsic defects induced by larger tensile strain, which is hardly reduced by the annealing process. It is found that Raman spectra of our samples contain a peak at about $690 cm^{-1}$. This peak is observed in both LCMO1 and LCMO2 films. According to previous reports on bulk and film LCMO samples, this high frequency mode is unassigned and may be related to the Ca doping, which originates from impurity^{38,39,51}. There are mainly two models in previous reports. In the first model, because this peak often presents in spectra of annealed $LaMnO_3$ samples and disappears in those polished samples⁵². It is maybe a sign of simple oxides like that of lanthanum or manganese originated from long-term degradation of the sample surface. In films on STO and MgO, this peak has a higher intensity, which suggests a more strongly degradation of these film's surface. However, the dependence of strain for this mode observed in our samples is hardly to explain within the above model. The frequency of this mode hardens when the sign of strain changes from tensile to compressive. The ideal epitaxy is preserved only within about the first 25 nm from the substrate-film interface²⁷. The strain releases with increasing of thickness. If this mode is a representation of simple oxides on the sample surface, the strain effect should be small. The strong dependence of strain for this mode suggests that this mode should not relate with the oxides on the sample surface. Another reasonable explanation of this peak could be the second-order Raman scattering^{52,53}. The comparable intensity of the second-order Raman spectra indicates both a relatively small distortion of a nearly cubic lattice and a disorder present in the perovskite structure. However, according to the XRD pattern shown above, the lattice distortion of film on MgO is a least one. In addition, it is hardly to be considered as a second-order due to such a high relative intensity of this peak in film on STO and MgO. According to the above discussion, we consider that this new peak is correlated with the interaction between lattice and substrate. This additional higher frequency mode is also observed in $Pr_{1-x}Ca_xMnO_3$ samples, caused by the lowering of the symmetry as a result of unit cell doubling along the a axis^{29,54}. Therefore, one reasonable possibility of the appearance of this mode comes from a lowering of the symmetry induced by strain. In addition, it is noticeable that this mode enhances and hardens in both LCMO1 and LCMO2 films with decreasing temperature. It seems to be independent of the Curie temperature (T_C) or the charge ordering temperature (T_{CO}), and to be decided by the strain simply. Therefore, we speculate that this mode reflect the information of the layers near the lattice-substrate interface. More detailed research about this peak need more experiments.

Similarly, the Raman spectra of $La_{0.5}Ca_{0.5}MnO_3$ films are also strongly depend on the type of strain. As shown in the Fig.3, obvious differences can be observed between the films on different substrates. The intensity of ω_1 is weak in LCMO2/LAO film with a compressive strain at

room temperature, and is the strongest in LCMO2/STO sample with a tensile strain, then is the most weak in film on MgO. The frequency changes complexly with decreasing of temperature (see Fig. 6). Its behavior depends on the type of strain. The changes of ω_2 in LCMO2 films are similar to those of LCMO1, strongly depend on the type of strain. Some sharp peaks appeared at low temperatures suggests a lowering symmetry, as observed in $La_{0.5}Ca_{0.5}MnO_3$ bulk samples. It seems to imply a transition of CO state. The frequency of ω_4 softens as the strain changes from a compressive one to a tensile one. It is consistent with the change of spectra in film with $x = 0.33$. It further proves that ω_4 mode is correlated with the lattice-substrate mismatch, namely strain in films. In addition, ω_3 can be observed clearer only in STO sample due to the large tensile strain, which leads to more oxygen deficit in the film during the growth process. These oxygen deficits induce by larger tensile strain are intrinsical and hardly suppressed.

There is a relaxation of the strains from the interface towards the surface. And the Raman scattering probes mainly the surface. It is probably that we observe different effect from strain by varying the laser wavelength. Unfortunately, we can not change the laser wavelength because of the limit of equipment. In our case, the thicknesses of the films are same. Thus, our discussion did not refer to the thickness of the films.

C. Effect of Ca Concentration

We compared the Raman spectra of samples with different Ca contents ($x = 0.33$ and 0.5) on the same substrate at different temperatures. It should be noticed that the out-of-plane lattice parameter decreases as Ca concentration increases in films on STO and MgO. While the lattice parameter increases in film on LAO. This difference in the change of lattice is induced by the different type strain in each film. In the film on LAO, the increase of out-of-plane lattice parameter with the increase of Ca concentration is induced by the following two reasons. One is the increase of Mn- O_{apical} -Mn angle. Liarokapis et al.⁴¹ had reported that the Mn- O_{apical} -Mn angle increases with the increase of Ca content in samples of higher Ca concentrations. This point can be proved by the softening of ω_1 in LCMO2/LAO compared with LCMO1/LAO. The other is the increase of Mn- O_{apical} bond length. Radaelli et al.⁵⁵ had reported that the distance between Mn ions and apical oxygens should increase with the decrease of A-site ionic radius $\langle r_A \rangle$ as $\langle r_A \rangle$ is less than 1.24 \AA . The $\langle r_A \rangle$ for $La_{0.7}Ca_{0.3}MnO_3$ is 1.205 \AA . In contrast, the out-of-plane lattice parameters of films grown on STO and MgO decrease as Ca concentration increases. This decrease of out-of-plane lattice parameter is also caused by two reasons. The first one is the decrease of the average ionic

radius at A-site. The second one is the decrease of JT distortions in $Mn^{3+}O_6$ octahedra ions due to the increase of Ca doping. ω_3 is pronounced in LCMO1/STO samples. In LCMO1 films, this pronounced peak indicates a higher oxygen deficit. As the Ca content increases to 0.5 , it becomes weak. The decrease in the intensity of this mode does not suggest a decrease of oxygen deficit. It can be explained by increasing the volume of domains with short-range charge/orbital-ordered. Therefore, with increasing Ca concentration, the Raman spectra change differently in the films on different substrate.

IV. CONCLUSIONS

Raman spectra of LCMO films grown on LAO(001), STO(001), and MgO(001) substrates were studied at different temperatures. According to the XRD pattern, there are a compressive strain for the films on LAO, a tensile strain for the films on STO and a slight strain for the films on MgO. The variations of Raman spectra with temperature, doping level and strain are studied. The effect of temperature and strain are hardly distinguished because the change of temperature is usually accompanied by a change of strain. In the films with Ca concentration of 0.33 , there is a PM-FM phase transition as temperature decreases. As the samples enter FM phase, the FWHM of ω_1 sharpens in LCMO1/LAO. The intensities of this tilted mode decreases dramatically in LCMO1 on STO and MgO. These changes of ω_1 are correlated with the spin-lattice coupling in spin-ordered FM state. For the high frequency ω_4 mode, an evident increase in their intensities occurs as temperature decreases. This seems to be a strain effect and is also observed in LCMO2 films. In the films with Ca concentration of 0.5 , Raman spectra change obviously with decreasing temperature. The changes indicate that the Raman spectra of films are strongly correlated with the disorder-order transition. The increase in the intensity of ω_3 is induced by the increase of oxygen defects in film on STO due to the large tensile strain in $La_{0.67}Ca_{0.33}MnO_3$ films. A unsigned mode appears at high frequency band, which depends on the strain strongly. As Ca concentration increases, the films on different substrates present different behaviors.

Acknowledgments

This work is supported by the Nature Science Foundation of China, by the Ministry of Science and Technology of China (Grant No. nkbrsf-g19990646) and by the Knowledge Innovation Project of Chinese Academy of Sciences for XHC, and in part by the State of Texas through the Texas Center for Superconductivity and Advanced Materials at the University of Houston for CLC.

- ¹ Amlan Biswas, M. Rajeswari, R.C. Srivastava, T. Venkatesan, R.L. Greene, Q. Lu, A.L. de Lozanne and A.J. Millis, *Phys. Rev. B* **63**, 184424(2001).
- ² J.C. Loudon, N.D. Mathur, and P.A. Midgley, *Nature* **420**, 797(2002).
- ³ B.B. Van Aken, O.D. Jurchescu, A. Meetsma, Y. Tomioka, Y. Tokura, and T.T.M. Palstra, *Phys. Rev. Lett.* **90**, 066403(2003).
- ⁴ J.H. So, J.R. Gladden, Y.F. Hu, J.D. Maynard, and Q. Li, *Phys. Rev. Lett.* **90**, 036103(2003).
- ⁵ S. Jin, T.H. Tiefel, M. McCormack, R.A. Fastnacht, R. Ramesh, and L.H. Chen, *Science* **264**, 413(1994).
- ⁶ J.M.D. Corey, M. Viret, and S. von Molnar, *Adv. Phys.* **48**, 167(1999).
- ⁷ M.N. Iliev, M.V. Abrashev, H.-G. Lee, V.N. Popov, Y.Y. Sun, C. Thomsen, R.L. Meng and C.W. Chu, *Phys. Rev. B* **57**, 2872(1998).
- ⁸ Yoshinori Tokura, *Colossal Magnetoresistive Oxides* (Gorden and Breach Science Publishers, The Netherlands, 2000).
- ⁹ Y. Tomioka, A. Asamitsu, Y. Moritomo, H. Kuwahara and Y. Tokura, *Phys. Rev. Lett.* **74**, 5108(1995).
- ¹⁰ A.P. Ramirez, P. Schiffer, S.-W. Cheong, C.H. Chen, W. Bao, T.T.M. Palstra, P.L. Gammel, D.J. Bishop and B. Zegarski, *Phys. Rev. Lett.* **76**, 3188(1996).
- ¹¹ C.H. Chen and S.-W. Cheong, *Phys. Rev. Lett.* **76**, 4042(1996).
- ¹² J.B. Goodenough, *Magnetism and the Chemical Bond* (John Wiley, New York, 1963).
- ¹³ C. Zener, *Phys. Rev.* **82**, 403 (1951).
- ¹⁴ A.J. Millis, *Phys. Rev. B* **53**, 8434(1996).
- ¹⁵ A.J. millis, *Nature* **392**, 147(1998).
- ¹⁶ A.J. Millis, P.B. Littlewood, and B.I. Shraiman, *Phys. Rev. Lett.* **74**, 5144(1995).
- ¹⁷ K. Steenbeck and R. Hiergeist, *Appl. Phys. Lett.* **75**, 1778(1999).
- ¹⁸ M. R. Ibarra, P. A. Algarabel, C. Marquina, J. Blasco and J. Garcia, *Phys. Rev. Lett.* **75**, 3541(1995).
- ¹⁹ G. Campillo, A. Berger, J. Osorio, J.E. Pearson, S.D. Bader, E. Baca, and P. Prieto, *J. Magn. And Magn. Mater.* **237**, 61(2001).
- ²⁰ J. M. De Teresa, M. R. Ibarra, J. Blasco, J. Garcia, C. Marquina and P. A. Algarabel, Z. Arnold, K. Kamenev, C. Ritter, R. von Helmolt, *Phys. Rev. B* **54**, 1187(1996).
- ²¹ R. von Helmolt, J. Wecker, B. Holzapfel, L. Schultz, K. Samwer, *Phys. Rev. Lett.* **71**, 2331(1993).
- ²² W. Prellier, Ph. Lecoewr and B. Mercey, *J. Phys.:Condens Matter* **13**, R915(2001).
- ²³ H.S. Wang, E. Wertz, Y.F. Hu, Qi Li, D.G. Schlom, J. Appl. Phys. **87**, 7409(2000).
- ²⁴ H.S. Wang, Qi Li, Kai Liu, C.L. Chen, *Appl. Phys. Lett.* **74**, 2212(1999).
- ²⁵ Qi Li, H.S. Wang, Y.F. Hu, E. Wertz, *J. Appl. Phys.* **87**, 5573(2000).
- ²⁶ A. Miniotas, A. Vailionis, E.B. Svedberg, U.O. Karlsson, *J. Appl. Phys.* **89**, 2134(2001).
- ²⁷ C.J. Lu, Z.L. Wang, C. Kwon and Q.X. Jia, *J. Appl. Phys.* **88**, 4032(2000).
- ²⁸ Amlan Biswas, M. Rajeswari, R. C. Srivastava, Y. H. Li, T. Venkatesan, R. L. Greene and A. J. Millis, *Phys. Rev. B* **61**, 9665(2000).
- ²⁹ A. Tatsi, E.I. Papadopoulou, D. Lampakis, E. Liarokapis, W. Prellier, and B. Mercey, *Phys. Rev. B* **68**, 24432(2003).
- ³⁰ N.G. Schmahl, J. Barthel, G.F. Eikerling, *Z. Anorg. Allg. Chem.* **332**, 230 (1964).
- ³¹ N. D. Mathur, M. -H. Jo, J. E. Evetts and M. G. Blamire *J. Appl. Phys.* **89**, 3388(2001).
- ³² M.V. Abrashev, J. Bäckström, L. Börjesson, M. Pissas, N. Kolev, and M.N. Iliev, *Phys. Rev. B* **64**, 144429(2001).
- ³³ M. Bibes, S. Valencia, Ll. Balcells, B. Martinez, J. Fontcuberta, M. Wojcik, S. Nadolski and E. Jedryka, *Phys. Rev. B* **66**, 134416(2002).
- ³⁴ J. Wollschläger, D. Erdös, K. M. Schröder, *Surf. Sci.* **402-404**, 272(1998).
- ³⁵ L. Chen, C.L. Chen, X. Chen, W. Donna, Y. Lin, S.W. Liu, D.X. Huang, and A.J. Jacobson, *Appl. Phys. Lett.* **83**, 4737(2003).
- ³⁶ L. Martín-Carró n, A. de André s, M.J. Martínez-Lope, M.T. Casais, and J.A. Alonso, *Phys. Rev. B* **66**, 174303(2002).
- ³⁷ M.V. Abrashev, V.G. Ivanov, M.N. Iliev, R.A. Chakalov, R.I. Chakalova, and C. Thomsen, *Phys. Stat. Sol.* **215**, 631(1999).
- ³⁸ V.B. Podobedov, D.B. Romero, A. Weber, J.P. Rice, R. Schreekala, M. Rajeswari, R. Ramesh, T. Venkatesan, and H.D. Drew, *Appl. Phys. Lett.* **73**, 3217(1998).
- ³⁹ N. Malde, P.S.I.P.N. de Silva, A.K.M. Akther Hossain, L.F. Cohen, K.A. Thomas, J.L. MacManus-Driscoll, N.D. Mathur and M.G. Blamire, *Solid State Commun.* **105**, 643(1998).
- ⁴⁰ M.V. Abrashev, J. Bäckström, L. Börjesson, V.N. Popov, R.A. Chakalov, N. Kolev, R.-L. Meng and M.N. Iliev, *Phys. Rev. B* **65**, 184301(2002).
- ⁴¹ E. Liarokapis, Th. Leventouri, D. Lampakis, D. Palles, J.J. Neumeier, and D.H. Goodwin, *Phys. Rev. B* **60**, 12758(1999).
- ⁴² V. Dediu, C. Ferdeghini, F.C. Maticotta, P. Nozar and G. Ruani, *Phys. Rev. Lett.* **84**, 4489(2000).
- ⁴³ M.N. Iliev and M.V. Abrashev, *J. Raman Spectrosc.* **32**, 805(2001).
- ⁴⁴ V.A. Amelichev, B.Güttler, O.Yu. Gorbenko, A.R. Kaul, A.A. Bosak, and A.Yu. Ganin, *Phys. Rev. B* **63**, 104430(2001).
- ⁴⁵ J.C. Irwin, J. Chrzanowski, and J.P. Franck, *Phys. Rev. B* **59**, 9362(1999).
- ⁴⁶ M.N. Iliev, M.V. Abrashev, V.N. Popov and V.G. Hadjiev, *Phys. Rev. B* **67**, 212301(2003).
- ⁴⁷ M.V. Abrashev, A.P. Litvinchuk, M.N. Iliev, R.L. Meng, V.N. Popov, V.G. Ivanov, R.A. Chakalov and C. Thomsen, *Phys. Rev. B* **59**, 4146(1999).
- ⁴⁸ S. Yoon, H.L. Liu, G. Schollerer, S.L. Cooper, P.D. Han, D.A. Payne, S.-W. Cheong, and Z. Fisk, *Phys. Rev. B* **58**, 2795(1998).
- ⁴⁹ P.G. Radaelli, D.E. Cox, M. Marezio, S.W. Cheong, *Phys. Rev. B* **55**, 3015(1997).
- ⁵⁰ E. Granado, N.O. Moreno, A. García, J.A. Sanjurjo, C. Rettori, I. Torriani, S.B. Oseroff, J.J. Neumeier, K.J. McClellan, S.W. Cheong and Y. Tokura, *Phys. Rev. B* **58**, 11435(1998).
- ⁵¹ A.E. Pantoja, H.J. Trodahl, R.G. Buckley, Y. Tomioka and Y. Tokura, *J. Phys.: Condens. Matter* **13**, 3741(2001).
- ⁵² V.B. Podobedov, A. Weber, D.B. Romero, J.P. Rice and

H.D. Drew, Phys. Rev. **B 58**, 43(1998).

⁵³ V.B. Podobedov, A. Weber, D.B. Romero, J.P. Rice and H.D. Drew, Solid State Commun. **105**, 589(1998).

⁵⁴ D.E. Cox, P.G. Radaelli, M. Marezio and S.-W. Cheong, Phys. Rev. **B 57**, 3305(1998).

⁵⁵ P.G. Radaelli, G. Iannone, M. Marezio, H.Y. Hwang, S-W. Cheong, J.D. Jorgensen, and D.N. Argyriou, Phys. Rev. **B 56**, 8265(1997).

⁵⁶ E.S. Vlahov, R.A. Chakalov, R.I. Chakalova, K.A. Nenkov, K. Dörr, A. Handstein, K.H. Müller, J. Appl. Phys. **83**, 2152(1998).

FIGURE CAPTIONS

Color online: Figure 1: X-ray diffraction patterns for $La_{1-x}Ca_xMnO_3$ films grown on three substrates with $x = 0.33$ and 0.5 , respectively.

Color online: Figure 2: Raman spectra of $La_{0.67}Ca_{0.33}MnO_3$ films on different substrates at the temperatures of 293, 260, 240, 220, 200, and 100 K. In Fig. 2a, the strong feature at about 486 cm^{-1} is

the LAO substrate peak identified by asterisks. Insets in Fig. 2 show the temperature dependence of magnetic moment for films on LAO, STO and MgO, respectively.

Color online: Figure 3: Raman spectra of $La_{0.5}Ca_{0.5}MnO_3$ films on different substrates at the temperatures of 293, 250, 200, 180, 160, 140, 100, and 83 K. In Fig. 3a, the strong feature at about 486 cm^{-1} is the LAO substrate peak identified by asterisks.

Color online: Figure 4: Raman spectra of as-grown and annealed LCMO1 films on STO and MgO, and LCMO2 film on LAO, respectively.

Color online: Figure 5: Temperature dependence of Raman shift of ω_2 , ω_3 and ω_4 for LCMO1 films.

Color online: Figure 6: Temperature dependence of Raman shift of ω_2 and ω_4 for LCMO2 films.

TABLE I: The out-of-plane lattice parameters of films and substrates estimated from XRD pattern data and references^{23,30,31,32}.

Substrate	Substrates		Films	
	Exp (Å)	Ref (Å)	$La_{0.67}Ca_{0.33}MnO_3$ (3.86 Å)(Å)	$La_{0.5}Ca_{0.5}MnO_3$ (3.84 Å)(Å)
$LaAlO_3$	3.7916	3.79	3.8822	3.8994
$SrTiO_3$	3.9026	3.905	3.8394	3.8036
MgO	4.2251	4.211	3.8666	3.8466

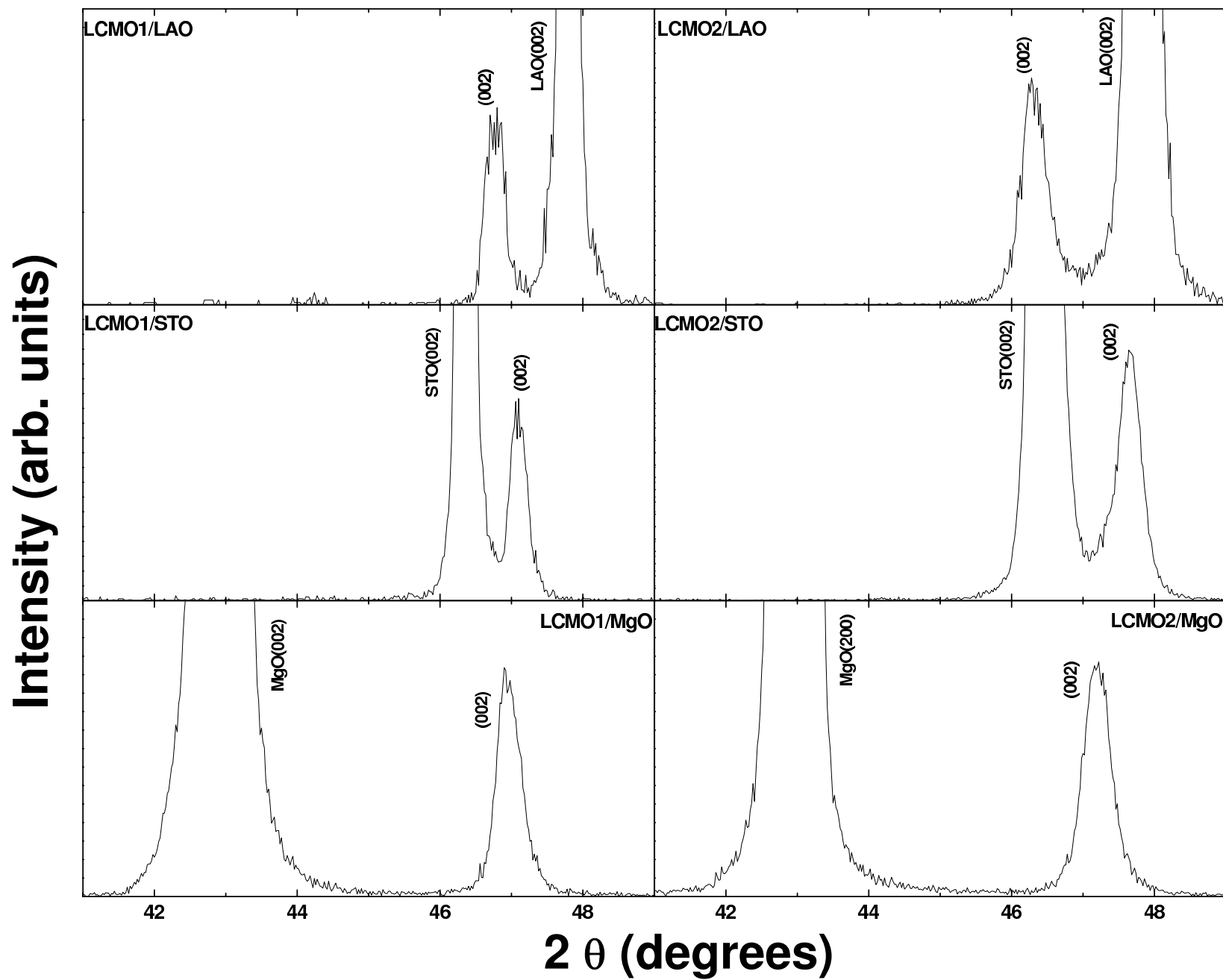


Figure 1

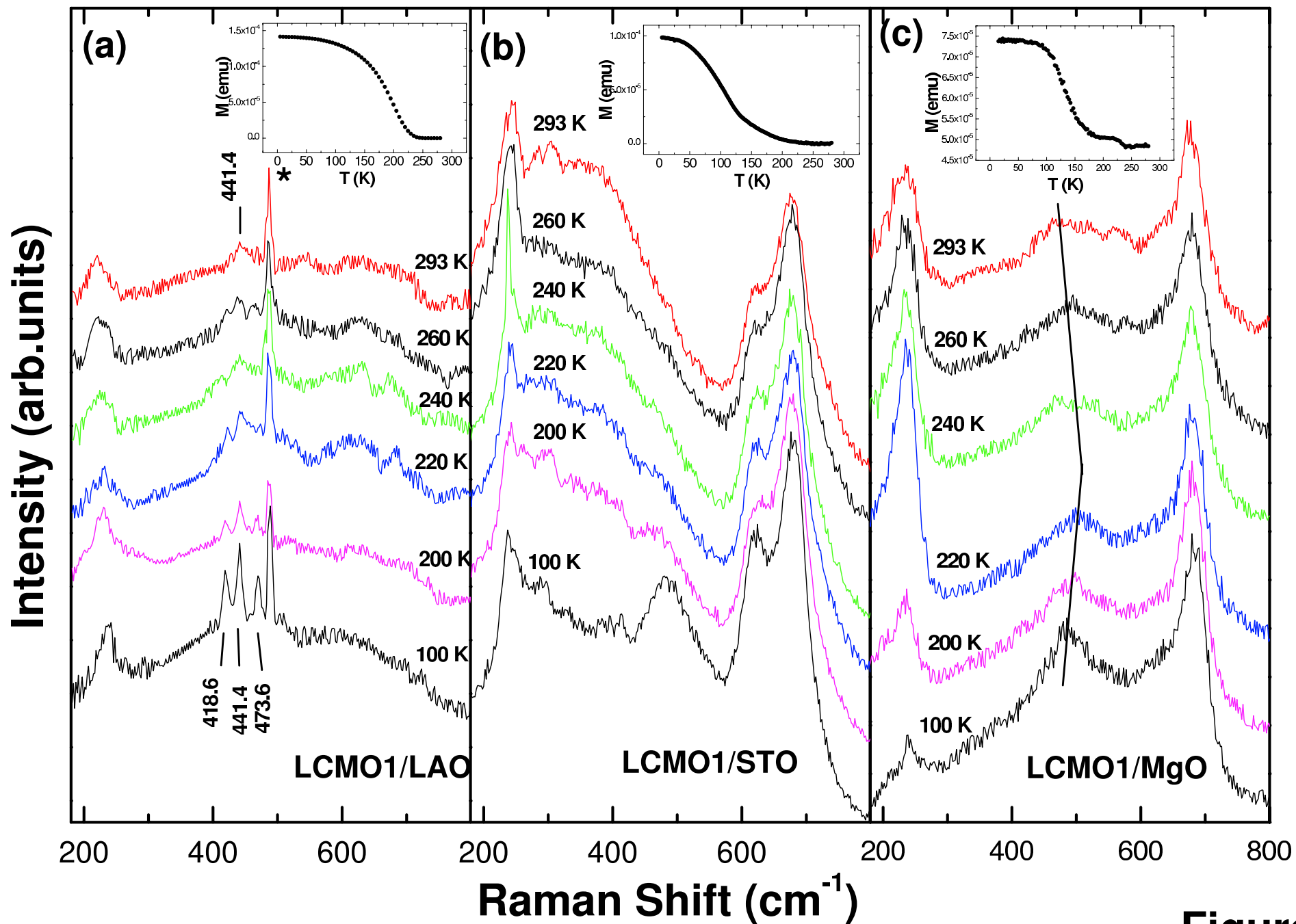


Figure 2

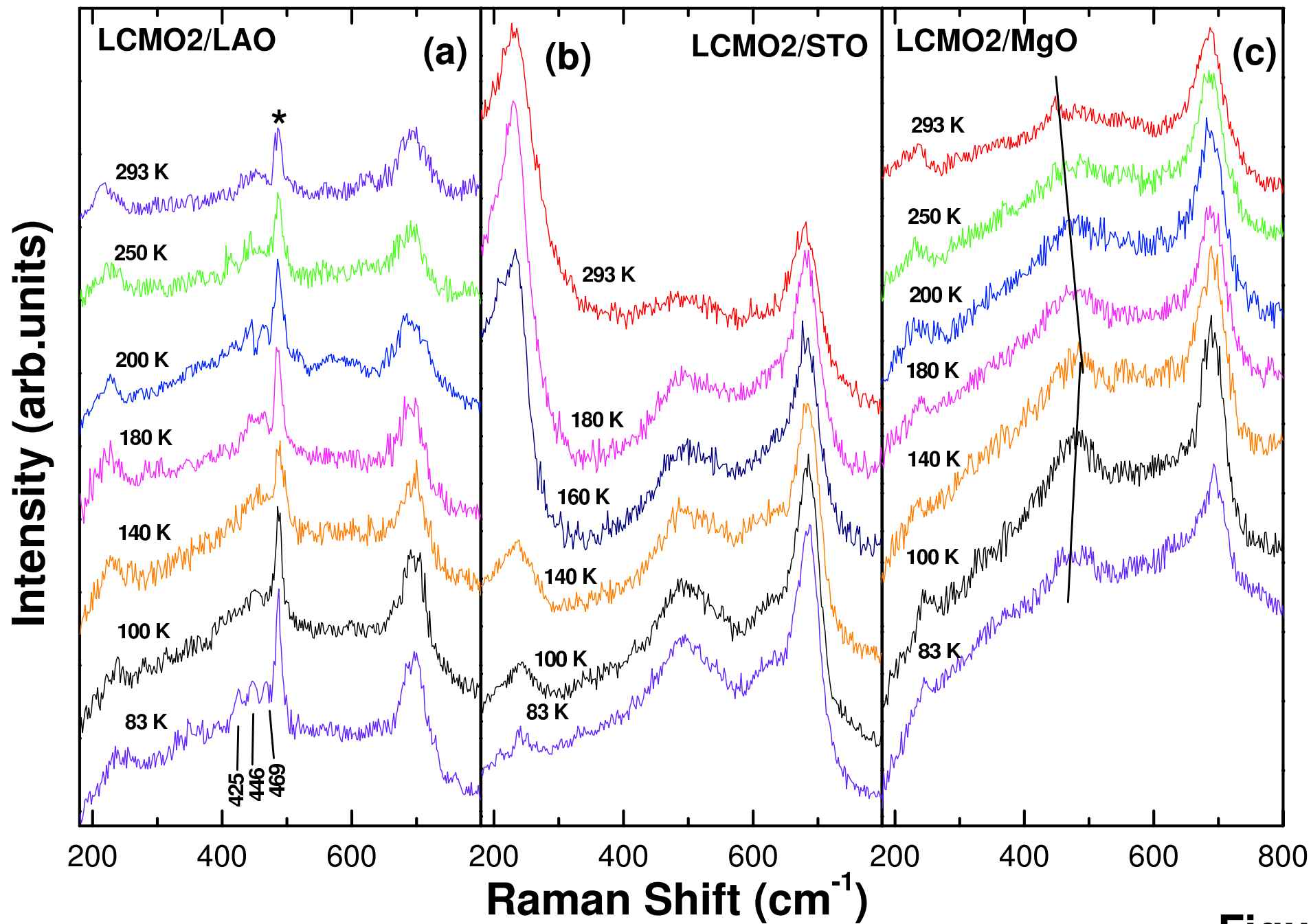


Figure 3

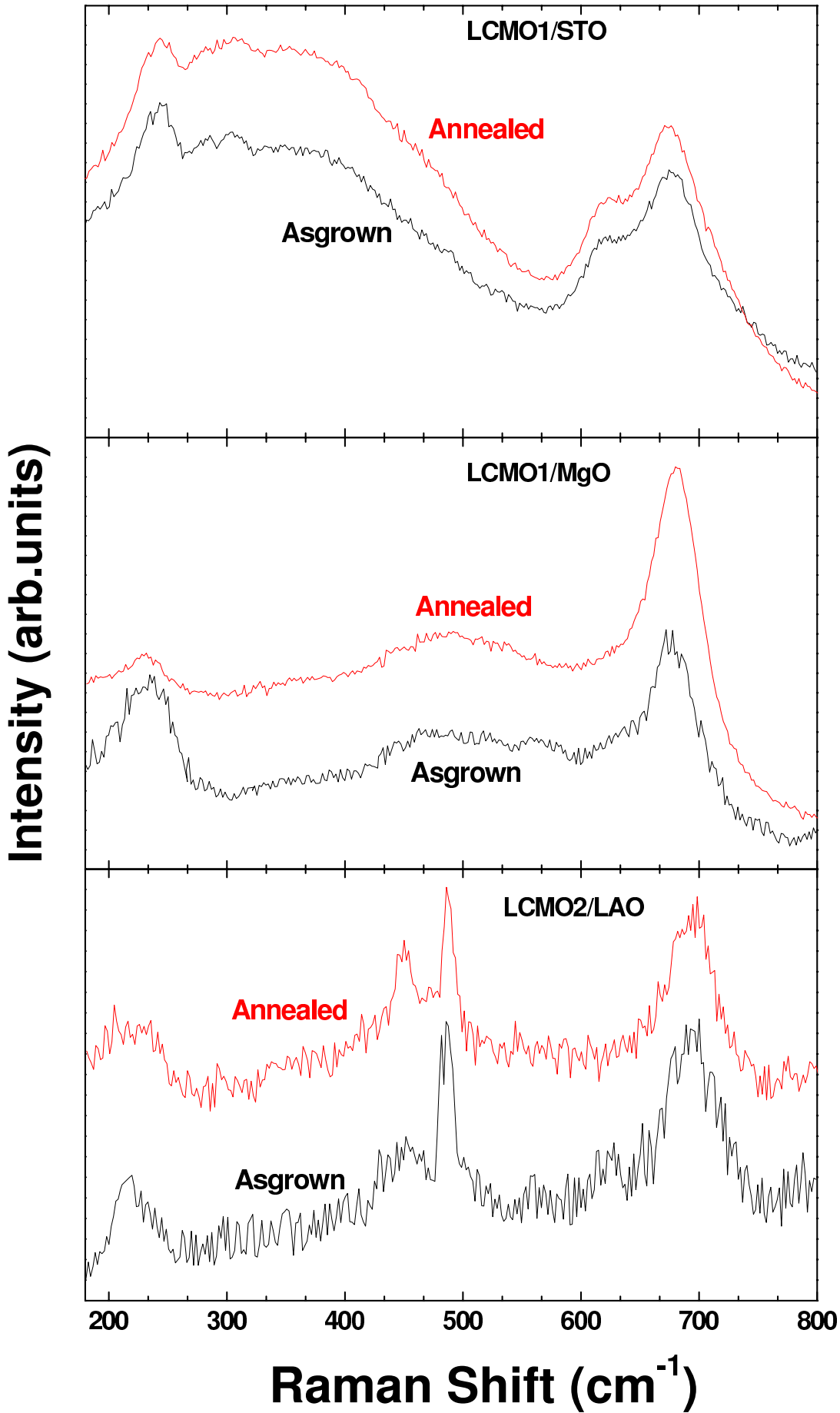


Figure 4

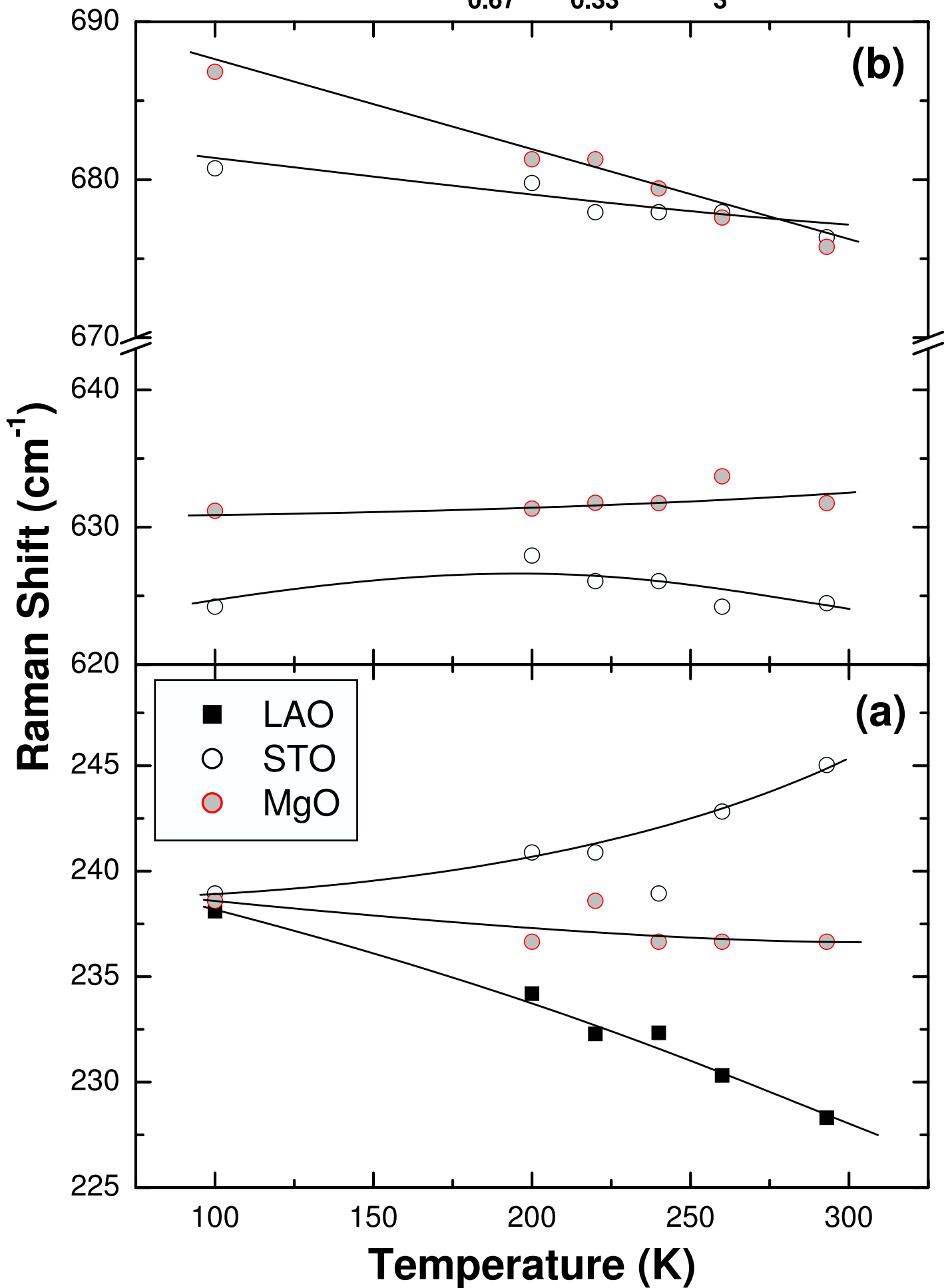


Figure 5

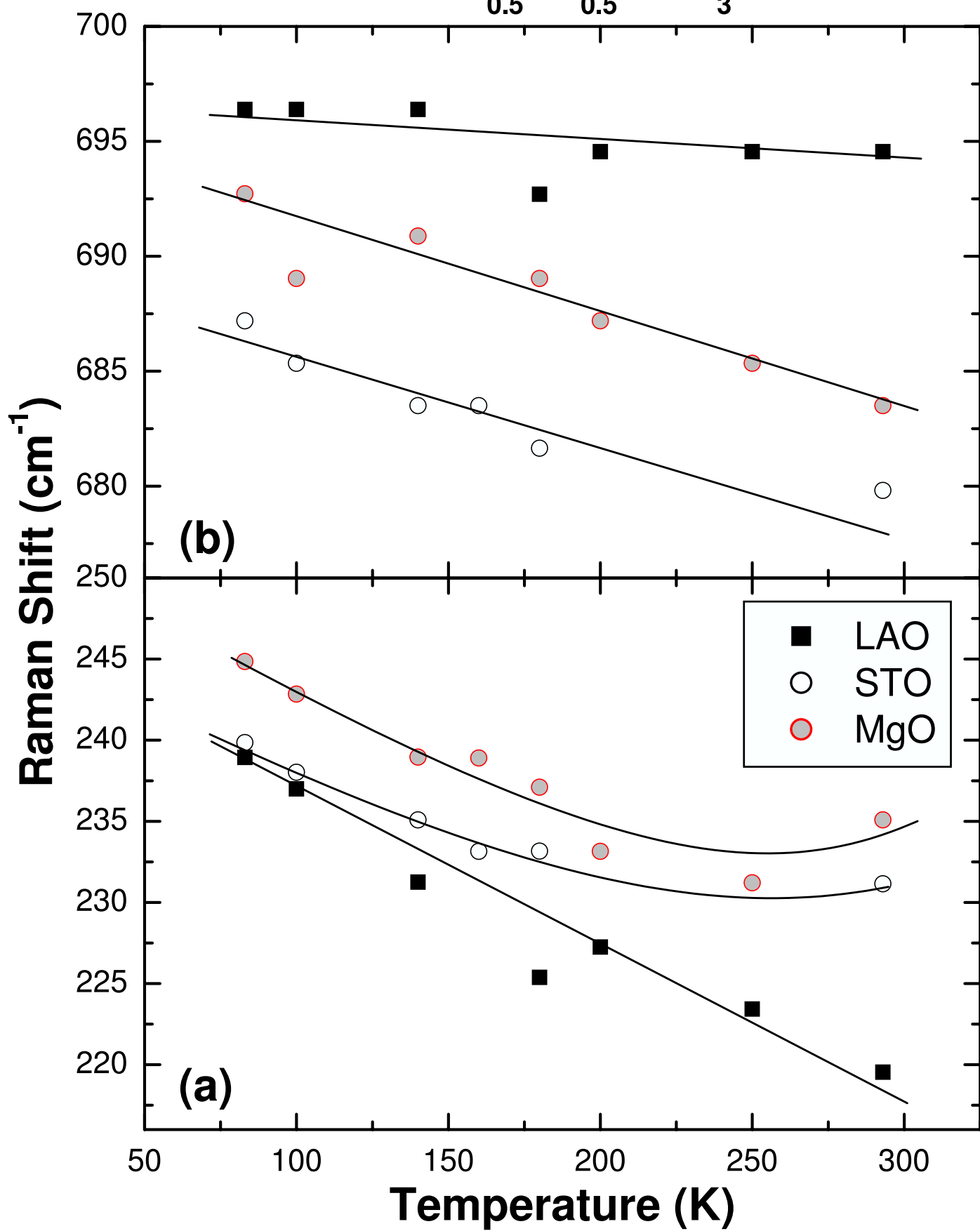


Figure 6